We are glad that all reviewers like our work and we thank all of them for their constructive comments. We have addressed the points raised by them as detailed below.

SC1

Comment 1. Interestingly, at intermediate distances the opposite effect can occur too, i.e. the total PRE can become slower than expected based on the simple Solomon equation. Is this due to NOE contacts with protons located at greater distance from the paramagnetic centre?

As noticed, at intermediate distances the total PRE can actually become slightly slower than expected from the Solomon equation. This is indeed caused by the dipole-dipole interactions with protons at larger distances from the paramagnetic metal, which cause "magnetization losses" from the closer to the farther protons. This is clarified by an additional simple simulation where 6 protons are placed along a straight line at 10, 12, 14, 16, 18 and 20 Å from a gadolinium ion. The results of the simulation are shown in the figures below. The magnetization of the proton at 10 Å recovers its equilibrium value slower than predicted from an exponential behavior, so that the monoexponential fit provides a longer relaxation time. The figure also shows (black dotted lines) the magnetization curves expected from the Solomon equation for the two protons at 10 and 20 Å. Clearly the first points of the magnetization recovery for the proton at 10 Å agree with the relaxation rate predicted by the Solomon equation. This comment has been introduced in the revised version, and the figures below have been added in the Supplement (Fig. S1).

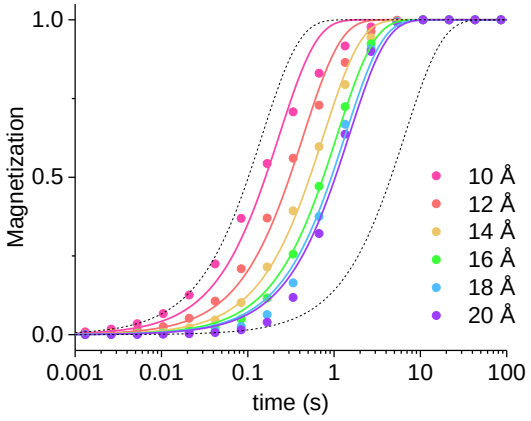

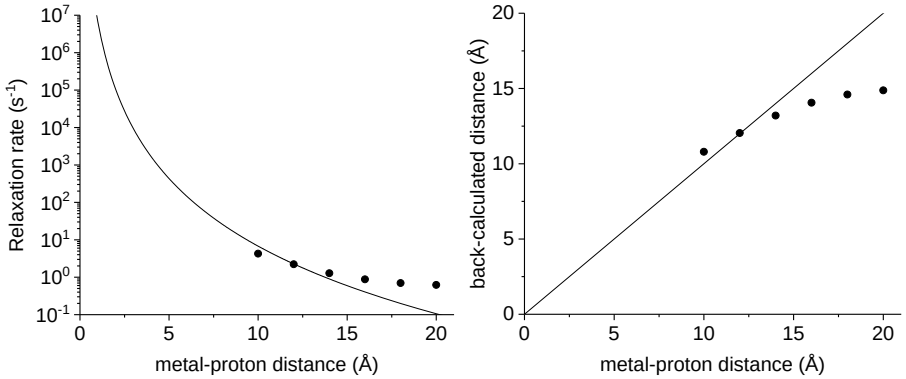

Figure S1. Calculated magnetization recovery for 6 protons placed along a straight line at 10, 12, 14, 16, 18 and 20 Å from a gadolinium ion, at 700 MHz (upper panel). The black dotted lines show the (monoexponential) behavior predicted from the Solomon equation for the two protons at 10 and 20 Å. The magnetization data calculated for the 6 protons are clearly not monoexponential. The monoexponential fits (solid colored lines) provide the relaxation rates and the back-calculated distances shown in the lower panels.

Comment 2. Can the authors predict what the situation would be like for backbone amide protons in a perdeuterated protein in H_2O, where the only protons are the amide protons from the backbone and side chains (also allowing the presence of hydroxyl protons)? What would the situation be like if the methyls of isoleucine, valine and leucine are protonated whereas the rest of the protein is perdeuterated?

We have performed the suggested calculations. As shown in the new Fig. S3A, amide and hydroxyl protons in perdeuterated conditions almost recover the rates predicted by the Solomon equation, although a slight smaller distance can anyway be calculated for protons at more than 20 Å from the paramagnetic metal. Methyl protons fully recover the Solomon behavior if the rest of the protein is perdeuterated (Fig. S3C). These plots have been added to the Supplement.

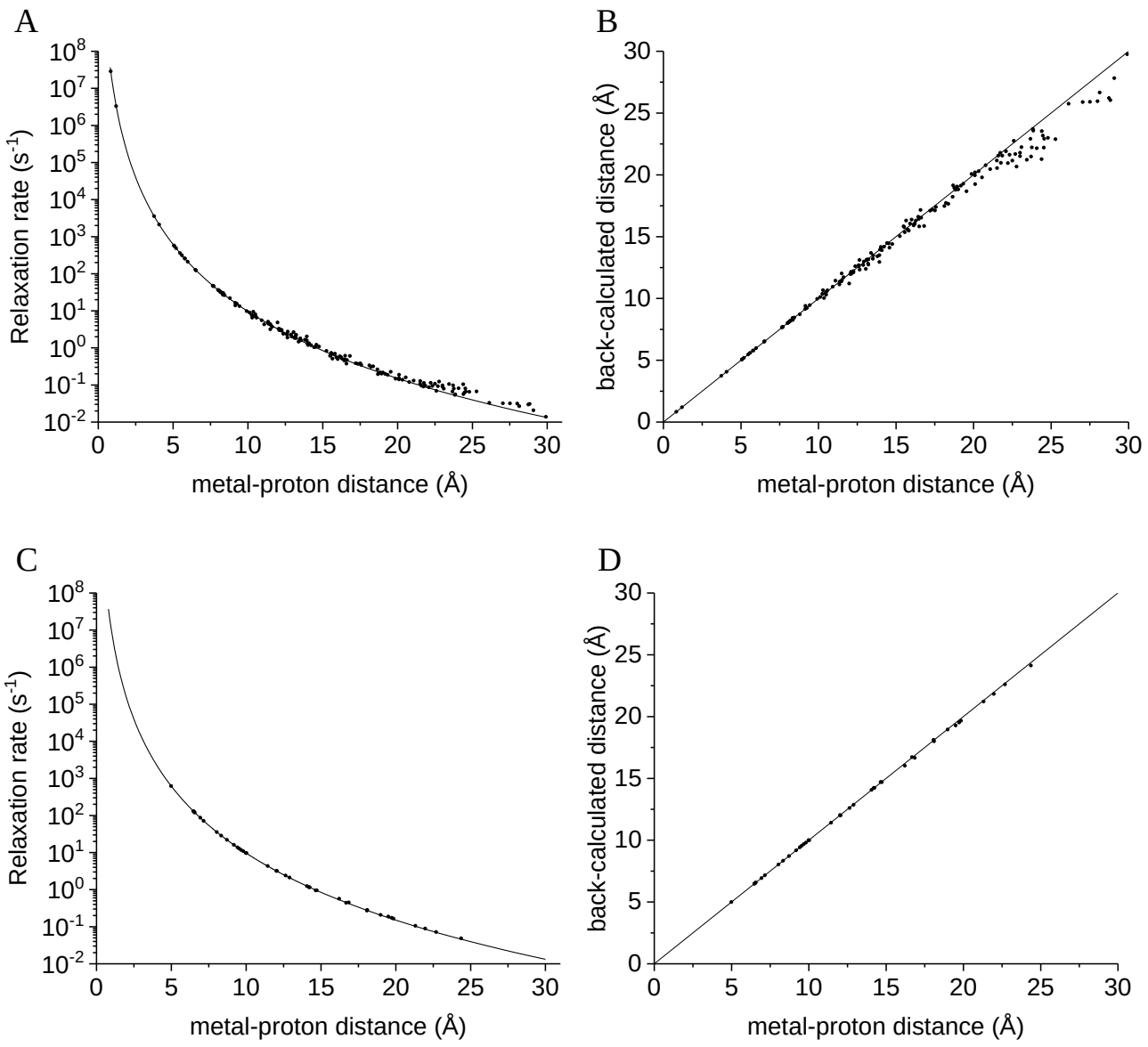

Figure S3. (A) Paramagnetic relaxation rates calculated at 500 MHz for Cu^{2+}-plastocyanin exchangeable (amide and hydroxyl) protons, in perdeuterated conditions. The line indicates the rates predicted with the Solomon equation. (C) Paramagnetic relaxation rates for isoleucine, leucine and valine methyl protons, assuming perdeuteration of all other hydrogens. (B and D) Agreement between metal-proton distances as measured in the PDB 2GIM structure and back-calculated from the predicted R_1 shown in panels A and C, respectively.

Comment 3. Line 136: exchange rates usually are expressed in s-1, not seconds.

In the revised version we have written "with an exchange rate of 10^4 s^{-1}". Thank you for having pointed this out.

SC2

The CORMA program as modified by the authors clearly is very useful. Would it be possible to install the software in the NMRbox provided by Jeffrey Hoch to make it generally accessible? This would not only be helpful for others but also increase the impact and citation rate of the present article. While the original CORMA software was developed many years ago in the group of Tom James at UCSF, it may be possible to obtain permission to make the new version accessible in this way?

We have written to the authors of CORMA and, if not forbidden, we are going to allow free access to the software from the CERM web site.

RC2

-It is not fully clear from the main text what the authors mean by "calculated rates". The authors use the adapted CORMA approach, they compute the evolution of the magnetization from Eq. 4. After this, one has to check Fig. S2 (not the main text) to find a fit of recovery to obtain the "calculated rate"? If so, are the recovery monoexponential? There seem to be some deviations in Figure S2.

It is correct that the recovery is not monoexponential. However, the "calculated rates" were indeed obtained from a monoexponential fit of the magnetization curves. We have now clarified this point immediately after the first paragraph of the Results and discussion section, by stating that "although for some nuclei the magnetization recovery curves deviate from monoexponential functions as expected (see below), the relaxation rates were calculated for simplicity as the rate constants of the assumed monoexponential time-dependences of the magnetization curves".

-In the discussion of Figure 1, the authors should make it more clear whether the effect discussed is due to cross-relaxation with faster relaxing protons (a "selective T_1" effect) and not simply the contribution of nucleus dipole-nucleus dipole interactions to relaxation (a "non-selective T1" effect).

Both indicated effects are effective when a non-selective pulse is applied, as done in our simulations. Most of the deviations is due to the different contributions from nucleus dipole-nucleus dipole interactions caused by the hyperfine coupling, but also cross relaxation effects are present. This can be checked by comparing the calculated rates from selective and non-selective experiments (see Figure below). This has been now clarified in the text (pag. 4).

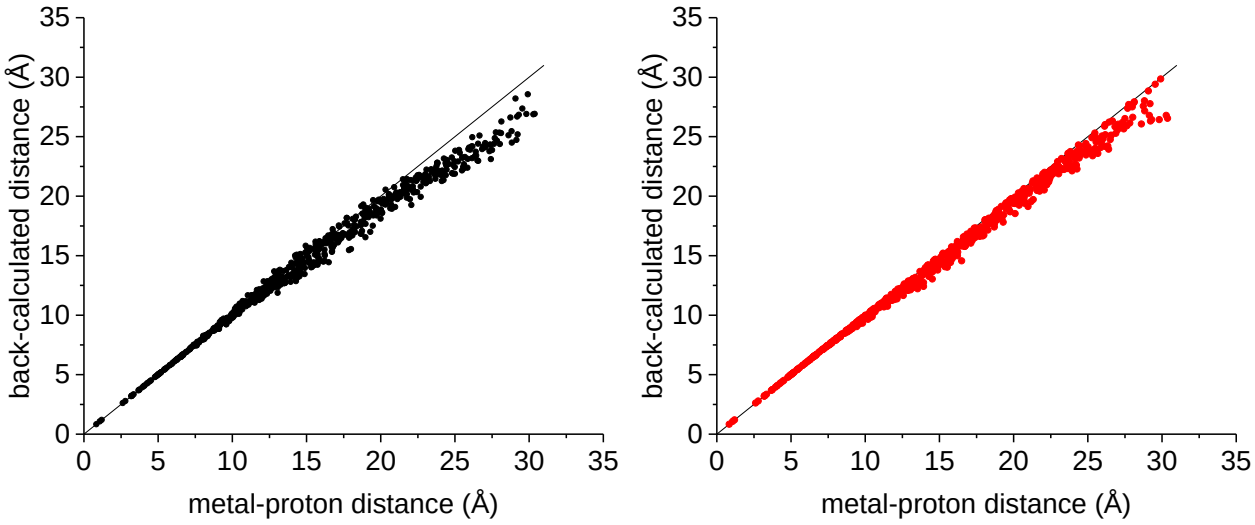

Agreement between metal-proton distances in Cu^{2+}-plastocyanin as measured in the PDB 2GIM structure and back-calculated from the predicted R_1 at 500 MHz: left panel, the relaxation rates are predicted by simulating a non-selective experiment (same plot shown in Figure 1 of the manuscript), right panel, the relaxation rates are predicted by simulating a selective experiment.

-In the light of the discussion between the authors and Gottfried Otting on a decrease of paramagnetic relaxation enhancements at intermediate distances, could this effect explain part of the surprising observations made by Flemming Hansen and Jens Led in their beautiful investigation of the blue copper site in Plastocyanin (JACS 2004)?

Although this effect may slightly contribute to the experimental observations by Hansen and Led, we do not expect sizable contributions in that case. In fact, whereas the effects that we calculate are sizable at 13 Å or farther from the metal, the deviations were observed by Hansen and Led at less than 10 Å from the metal.

-The authors rightfully refer the contribution to relaxation from interactions with electrons to the seminal work of Solomon by mentioning the "Solomon Equation". However, I find this expression possibly confusing, especially in the context of this investigation. The legacy of Ionel Solomon reached beyond the expression of relaxation in paramagnetic systems and it is widely accepted in NMR that the Solomon EquationS describe the evolution of magnetization in the presence of dipolar cross-relaxation, which is also perfectly relevant to this study. I believe that the authors should mention these Solomon Equations (introduced in the same Phys. Rev. 1955 article). It would be fantastic if the authors could

take this opportunity to clarify the Solomon Equation vs. Solomon Equations issue, possibly by referring to the former as the Bloombergen-Solomon Equation as some do in the literature.

We have now clarified (pag. 2) that we call Solomon equation the widely used equation provided by Solomon for paramagnetic solutions (Solomon, 1955), although in the same work Solomon also provided the coupled equations which include cross-relaxation terms and should be taken into account for treating the case of nucleus dipole-nucleus dipole interacting spins. We prefer not to refer to the Bloembergen-Solomon equation because it includes contributions from Fermi-contact relaxation, which are not considered in this work.

-I wonder if calculating the evolution of the magnetization would be easier with the use of the Homogeneous Master Equation (Levitt and di Bari 1992).

This could be possible, but we have preferred a more "classical" approach, to better control all steps in the implementation of the model.

-On lines 128-129, the authors mention that, in the absence of exchange, the bulk water relaxation rate is not altered by the interaction with the electron magnetic dipole. Is it true or is it an approximation since outer-sphere relaxation mechanisms are not the topic of this investigation?

Contributions from outer-sphere relaxation are not considered in this work because of the large distance of the water molecules from the paramagnetic center, and thus not included into the model. This has been now clarified in the text (pag. 6).

- I am not sure I understand exactly how the relaxation rates of the bulk calculated from the Solomon equation represented by dashed and solid lines in Figure 3 were calculated, what was included in each calculation.

The relaxation rates at 1 T (solid lines) and 3 T (dashed lines) are calculated from the Solomon relaxation rates $R_{1,M}$ of the exchangeable protons in the absence of any cross-relaxation terms, according to the relationship $R_{1\mathrm{bulk}} = R_{1\mathrm{dia}} + f(R_{1M}^{-1} + \tau_M)^{-1}$. This has been clarified in the caption of figure 3.

-In the spirit of Magnetic Resonance, it would be preferable that the authors publish the simulation code used in their study.

We have written to the authors of CORMA and, if not forbidden, we are going to allow free access to the software from the CERM web site.

Minor:

-On lines 32-34, the question of non-monoexponential evolution of polarizationin the presence of cross-relaxation could fill out volumes. The reference to the work of Banci and Luchinat is perfectly relevant

here but could be accompanied by a general reference to nuclear Overhauser effects (e.g. the already cited Solomon article or the textbook by Neuhaus and Williamson).

We agree to cite these more general references.

-Similarly, the "Furthermore" on line 33 could be replaced by "Indeed" or any other suggestion by the authors since cross-relaxation is the cause of non-monoexponentiality.

OK

-Including chemical exchange in the CORMA approach has been done in the past, for instance by Jayalakshmi and Rama Krishna (JMR 2002).

This work is now cited. Thank you for pointing it out.

-Many symbols are not defined in the main text. I may have missed some but could not find the definition of rho_i, k_i, sigma_ij, g_e, mu_B, B_0, gamma_i, tau_e, Delta_1, and tau_nu.

All these symbols are now defined (pag. 3).

-Unless this is a format requirement of Magnetic Resonance, I would suggest the authors use a first page with article title and authors list in the supplementary information document.

OK

RC3

I have a few simple suggestions for the authors.
- Line 37: There were a number of groups who examined multiple-spin effects on cross-relaxation rates using a complete rate matrix at the same time as Borgias and James, 1989. It would be nice to reference some of the other papers as well (e.g. Boelens and Kaptein, J Mag Res 1989; Olejniczak and Fesik J Mag Res 1986; co-workers and Gorenstein JACS 1990).

These references have been added as suggested.

- Line 55 and elsewhere: The use of "the CORMA approach" sounds like the approach is unique to the CORMA program, but that is somewhat misleading as other programs from other research groups utilize a complete relaxation rate-matrix approach. A more accurate phrase would be "the CORMA program" or "the complete rate-matrix approach."

The expression has been changed as suggested (complete relaxation rate-matrix approach)

- Eq 1: I could not see the definition for sigma in the main text. Although the definition does appear in the supplement, it should appear with equation 1.

Rho and sigma are now defined immediately after Eq. 1.

- Figure 1 and the description lines 92-100: The authors compare in fig 1a and 1c the apparent rates that would result from analyzing M'(t) in comparison to the actual Solomon relaxation rate, eqn 2. It would be helpful for the reader to articulate in the figures and text "apparent relaxation rate" or somehow differentiate a rate estimated from M'(t) versus the actual rates that appear in the rate matrix, eqn 1.

The expression "apparent relaxation rates" is now defined and used in the text and in the caption of Fig. 1.

- line 91: it is mentioned that Led and coworkers reported deviations in distances determined from analysis of experimental magnetization decay. Can the authors make a direct comparison of the computed results (fig 1) with the experimental data? For example, the theoretical back-calculated distances in 1b with the experimental distances calculated from the experimental longitudinal relaxation rates?

As suggested, we have now included in Fig. 1B the distances back calculated from the experimental rates collected by Led and coworkers for a direct comparison with computed data.

Typographical corrections:
- line 96: "Analogous behaviors are" should be "Analogous behavior is"
-line 98: "differ of orders" should be "differ by orders"
-line 170: "This occurs" is missing a subject noun. Perhaps "This contribution occurs" or "This transfer occurs"

Corrected, thank you!

Revisiting paramagnetic relaxation enhancements in slowly rotating systems: how long is the long range?

Giovanni Bellomo[1,2,$], Enrico Ravera[1,2], Vito Calderone[1,2], Mauro Botta[3], Marco Fragai[1,2], Giacomo Parigi[1,2], Claudio Luchinat[1,2]

[1]Magnetic Resonance Center (CERM) and Department of Chemistry, University of Florence, via Sacconi 6, Sesto Fiorentino, Italy
[2]Consorzio Interuniversitario Risonanze Magnetiche di Metalloproteine (CIRMMP), Sesto Fiorentino, Italy
[3]Dipartimento di Scienze e Innovazione Tecnologica, Università del Piemonte Orientale "Amedeo Avogadro", Viale T. Michel 11, 15121, Alessandria, Italy
[$]Present address: Laboratory of Clinical Neurochemistry, Neurology Clinic, University of Perugia, Piazzale Lucio Severi 1/8, 06132 Perugia (PG), Italy

Correspondence to: Claudio Luchinat (luchinat@cerm.unifi.it)

Abstract. Cross relaxation terms in paramagnetic systems that reorient rigidly with slow tumbling times can increase the effective longitudinal relaxation rates of protons of more than one order of magnitude. This is evaluated by simulating the time evolution of the nuclear magnetization using a complete relaxation rate-matrix approach. The calculations show that the Solomon dependence of the paramagnetic relaxation rates on the metal-proton distance (as r^{-6}) can be incorrect for protons farther than 15 Å from the metal, and thus can originate sizable errors in R_1-derived distance restraints used, for instance, for protein structure determination. Furthermore, the chemical exchange of these protons with bulk water protons can enhance the relaxation rate of the solvent protons by far more than expected from the paramagnetic Solomon equation. Therefore, it may contribute significantly to the water proton relaxation rates measured at MRI magnetic fields in the presence of slow-rotating nanoparticles containing paramagnetic ions and a large number of exchangeable surface protons.

1 Introduction

Paramagnetic relaxation rates are largely applied for macromolecular structure determination, because they provide information on the distance of the macromolecule nuclei from the paramagnetic metal ion, as well as in the field of magnetic resonance imaging (MRI) (Bertini et al., 2017). Image contrast in MRI is in fact largely determined by the different nuclear relaxation rates of the water protons present in the different tissues of the human body (Koenig and Brown III, 1990). However, in many cases the intrinsically low difference among relaxation rates of water protons in different tissues requires the use of contrast agents to highlight the presence of pathological conditions (Aime et al., 2006, 2019; Wahsner et al., 2019). In this study, we explore the possibility to increase the efficacy of a paramagnetic molecule as MRI contrast agent by exploiting cross relaxation effects.

The relaxation rate is defined assuming a monoexponential time-dependence of the magnetization during the recovery of its equilibrium conditions after a perturbation. However, the presence of dipole-dipole coupled nuclear spins can result in magnetization time-dependences which are not monoexponential (Banci and Luchinat, 1998; Neuhaus and Williamson, 1989; Solomon, 1955). ~~Furthermore~~Indeed, in the presence of multiple nuclei, the dipole-dipole coupling between the spins can cause exchange of magnetization from one to another, and this effect can propagate diffusively throughout the macromolecule (spin diffusion). This is a well-known, although often overlooked, feature, which can be correctly taken into account by complete relaxation rate-matrix analysis (Boelens et al., 1989; Olejniczak et al., 1986; Post et al., 1990) through programs like CORMA (Borgias et al., 1989).

In the presence of unpaired electron(s) (e.g.: radicals or paramagnetic metal complexes), the dominant dipole-dipole interaction for nuclear spins is often that with the spin of the unpaired electron(s), even if the latter is much farther than other neighboring nuclei. In this case, the corresponding paramagnetic relaxation rate constant is described by the Solomon equation for paramagnetic solutions (Solomon, 1955), which dictates a dependence of the paramagnetic relaxation rate on the inverse sixth power of the distance of the nuclear spin from the paramagnetic center (r^{-6}). However, the presence of multiple dipole-dipole interactions between nuclei close to one another is expected to considerably increase the nuclear relaxation rate. Hereafter, we call Solomon equation the widely used equation provided by Solomon for paramagnetic solutions (Solomon, 1955), although in the same work Solomon also provided the coupled equations which include cross-relaxation terms and should be taken into account for treating the case of nucleus dipole-nucleus dipole interacting spins.

We have here modified the program CORMA to calculate i) the longitudinal relaxation rates of protons in molecules with known structure, in the presence of paramagnetic ions, taking into account all cross-relaxation effects, and ii) the longitudinal relaxation rates of the bulk water protons, in the presence of some protons of the molecule in exchange with the bulk (Libralesso et al., 2005; Ravera et al., 2013). This model allowed us to calculate the deviations of the relaxation enhancements with respect to the values predicted by the paramagnetic Solomon equation on the basis of the metal-proton distances, and thus the gain in relaxation rate values due to the network of the dipole-dipole interactions.

2 Complete relaxation matrix analysis

If a macromolecule is dissolved in solution, the longitudinal relaxation rate of the solvent nuclei increases with respect to the value of the pure solvent molecules due to the presence, at the surface of the macromolecule, of solvent molecules in chemical exchange with bulk solvent molecules. The correlation time for the dipole-dipole interactions involving these solvent molecule nuclei is the shortest between the reorientation time of the macromolecule (τ_R) and their lifetime ($\tau_{M,i}$).

Using the ~~CORMA~~ complete relaxation rate-matrix approach (Borgias et al., 1989; Jayalakshmi and Rama Krishna, 2002) (see supplement), the relaxation rates of the solvent molecule nuclei interacting with the macromolecule and of the bulk solvent molecule nuclei can be calculated by including in the relaxation matrix as many extra rows and columns as the number of nuclei belonging to the interacting solvent molecules, and an additional row and column relative to bulk solvent

nuclei. Assuming M solvent nuclei interacting with the macromolecule (composed of N nuclei), and using a "normalized" magnetization for the bulk nuclei, $\mathbf{M'} = \begin{pmatrix} M_z^I \\ \vdots \\ fM_z^B \end{pmatrix} = \begin{pmatrix} M_z^I \\ \vdots \\ \widetilde{M}_z^B \end{pmatrix}$, the relaxation matrix becomes (see supplement)

$$\mathbf{R'} = \begin{pmatrix} \rho_1 + k_1 + R_{1M,1} & \sigma_{12} & \cdots & \sigma_{1N} & \sigma_{1(N+1)} & \cdots & \sigma_{1(N+M)} & -k_1 \\ \sigma_{12} & \rho_2 + k_2 + R_{1M,2} & \cdots & \sigma_{2N} & \sigma_{2(N+1)} & \cdots & \sigma_{2(N+M)} & -k_2 \\ \vdots & \vdots & \ddots & \vdots & \vdots & \ddots & \vdots & \vdots \\ \sigma_{1N} & \sigma_{2N} & \cdots & \rho_N + k_N + R_{1M,N} & \sigma_{N(N+1)} & \cdots & \sigma_{N(N+M)} & -k_N \\ \sigma_{1(N+1)} & \sigma_{2(N+1)} & \cdots & \sigma_{N(N+1)} & \rho_{N+1} + k_{N+1} + R_{1M,N+1} & \cdots & \sigma_{(N+1)(N+M)} & -k_{N+1} \\ \vdots & \vdots & \ddots & \vdots & \vdots & \ddots & \vdots & \vdots \\ \sigma_{1(N+M)} & \sigma_{2(N+M)} & \cdots & \sigma_{N(N+M)} & \sigma_{(N+1)(N+M)} & \cdots & \rho_{N+M} + k_{N+M} + R_{1M,N+M} & -k_{N+M} \\ -fk_1 & -fk_2 & & -fk_N & -fk_{N+1} & & -fk_{N+M} & \rho_B + f\sum_i k_i \end{pmatrix} \quad (1)$$

where $k_i = (\tau_{M,i})^{-1}$ are the exchange rate constants, f is the ratio between the macromolecular concentration and the solvent molecule nuclei concentration, ρ_i and σ_{ij} are the (diamagnetic) auto and cross-relaxation rates (see supplement), and ρ_B is the relaxation rate of bulk solvent nuclei in the absence of the macromolecule. In order to consider the contribution to relaxation caused by a paramagnetic metal ion present in the macromolecule, the terms $R_{1M,i}$ appear in the diagonal elements of the relaxation matrix. They correspond to the Solomon paramagnetic relaxation rates

$$R_{1M,i} = \frac{2}{15}\left(\frac{\mu_0}{4\pi}\right)^2 \frac{\gamma_I^2 g_e^2 \mu_B^2 S(S+1)}{r_{iM}^6}\left[\frac{7\tau_{ci}}{1+\omega_S^2\tau_{ci}^2} + \frac{3\tau_{ci}}{1+4\omega_I^2\tau_{ci}^2}\right] \quad (2)$$

where S is the electron spin quantum number, $\omega_S^2 = g_e^2\mu_B^2 B_0^2$ ~~and ,~~ $\omega_I^2 = \gamma_I^2 B_0^2$ ~~and ,~~ the correlation time is given by $\tau_{ci}^{-1} = \tau_R^{-1} + \tau_e^{-1} + \tau_{Mi}^{-1}$, τ_e is the electron relaxation time, g_e is the electron g factor, μ_B is the electron Bohr magneton, γ_I is the nuclear magnetogyric ratio, and B_0 is the applied magnetic field. The relaxation matrix in Eq. 1 is not symmetric. However, we can define a symmetric matrix $\mathbf{R}_s = \mathbf{F}^{-1}\cdot\mathbf{R'}\cdot\mathbf{F}$, where

$$\mathbf{F} = \begin{pmatrix} 1 & 0 & \cdots & 0 \\ 0 & 1 & \cdots & 0 \\ \vdots & \vdots & \ddots & \vdots \\ 0 & 0 & \cdots & \sqrt{f} \end{pmatrix} \quad (3)$$

If $\boldsymbol{\lambda}_s$ is the diagonal matrix of the eigenvalues and $\boldsymbol{\chi}_s$ is the unitary eigenvector matrix of $\mathbf{R}_s$, the time evolution of the longitudinal magnetization is

$$\mathbf{M'}(t) - \mathbf{M'_{eq}} = \mathbf{F}\cdot\boldsymbol{\chi}_s\cdot\exp(-\boldsymbol{\lambda}_s t)\cdot\boldsymbol{\chi}_s^{-1}\cdot\mathbf{F}^{-1}\cdot(\mathbf{M'}(0) - \mathbf{M'_{eq}}) \quad (4)$$

3 Results and discussion

The relaxation rates of all protons belonging to a macromolecule containing a paramagnetic metal ion can be calculated using a modified version of the program CORMA (Borgias et al., 1989), called CORMA-PODS (COmplete Relaxation Matrix Analysis – Paramagnetic Or Diamagnetic Solutions). In summary, after diagonalization of the relaxation matrix in

Eq. 1, the time dependence of the longitudinal magnetization of all macromolecule protons as well as of bulk water protons can be calculated from Eq. 4 (with all elements of the vector $\mathbf{M'_{eq}}$ equal to 1), with all elements of the vector $\mathbf{M'}(0)$, describing the initial longitudinal magnetizations, equal to the same value (−1 or 0 to simulate an inversion recovery or a 90° pulse, respectively), assuming that a non-selective radiofrequency pulse is applied. Although for some nuclei the magnetization recovery curves deviate from monoexponential functions as expected (see below), the "apparent" relaxation rates were calculated for simplicity as the rate constants of the assumed monoexponential time-dependences of the magnetization curves.

3.1 Paramagnetic relaxation rates in high field NMR spectroscopy

We first checked whether cross relaxation effects can cause sizable deviations of the nuclear relaxation rates from the expected r^{-6} dependence predicted by the Solomon equation in paramagnetic proteins at high magnetic field. Since the experimental rates are used to back calculate, through the Solomon equation, the nucleus-metal distances to be employed as restraints for molecular structure determination, this would result in incorrect structural restraints.

A deviation between the correct metal-proton distances and those determined from the longitudinal relaxation rates was first experimentally observed by Led and coworkers (Ma et al., 2000) at 500 MHz for the protein plastocyanin, a copper(II) protein with a reorientation time of 6.2 ns and an electron relaxation time of 0.17 ns. Figure 1A shows the apparent paramagnetic relaxation enhancement of all plastocyanin protons in these conditions, calculated as the difference between the apparent rates obtained with including the paramagnetic metal and without it. The deviations from the Solomon behavior for many protons at distances larger than 15 Å result in metal-proton distances (Fig. 1B) somewhat smaller than the correct ones, in accordance with the experimental data. As already noted by Led, the experimental data tend to deviate more than predicted from CORMA. These deviations from the Solomon equation in the calculated data are due to both the different contributions from nucleus dipole-nucleus dipole interactions arising in the presence of the paramagnetic metal, and cross relaxation effects. A few protons at intermediate distances may also have slightly slower relaxation rates than expected from the Solomon equation. This is caused by the nucleus dipole-nucleus dipole interactions among protons at large distances from the paramagnetic metal, which cause "magnetization losses" from the closer to the farther protons, with clear deviations from a monoexponential magnetization recovery (see Fig. S1). Analogous behavior~~s~~ ~~are~~ is calculated for the catalytic domain of the protein matrix metalloproteinase 12 (Balayssac et al., 2008; Benda et al., 2016), by replacing the catalytic zinc ion with high spin cobalt(II), copper(II) or gadolinium(III) (Fig. S~~1~~2), although the electron relaxation rates of the different metals differ ~~of~~ by orders of magnitude. These deviations from the Solomon behavior are largely reduced or completely removed for amide and hydroxyl protons in perdeuterated conditions, and for (isoleucine, leucine and valine) methyl protons if the rest of the protein is perdeuterated (Fig. S3).

This analysis represents a warning to the use of distance restraints for the structural refinement of macromolecules, derived from experimental R_1 using the Solomon equation, for protons at distances farther than 15 Å from the paramagnetic metal.

On the other hand, these calculations are performed in the assumption of completely rigid molecules (except methyl jumps), which is clearly an unrealistic assumption for biomolecules. Internal mobility may actually reduce the deviations with respect to the Solomon predictions. Fast local mobility is in fact of paramount importance in determining the relaxation rates. If methyl protons were fixed, instead of jumping fast between different positions, the deviations from the Solomon behavior for protons at distances larger than 20 Å were in fact significantly larger (see Fig. 1C,D).

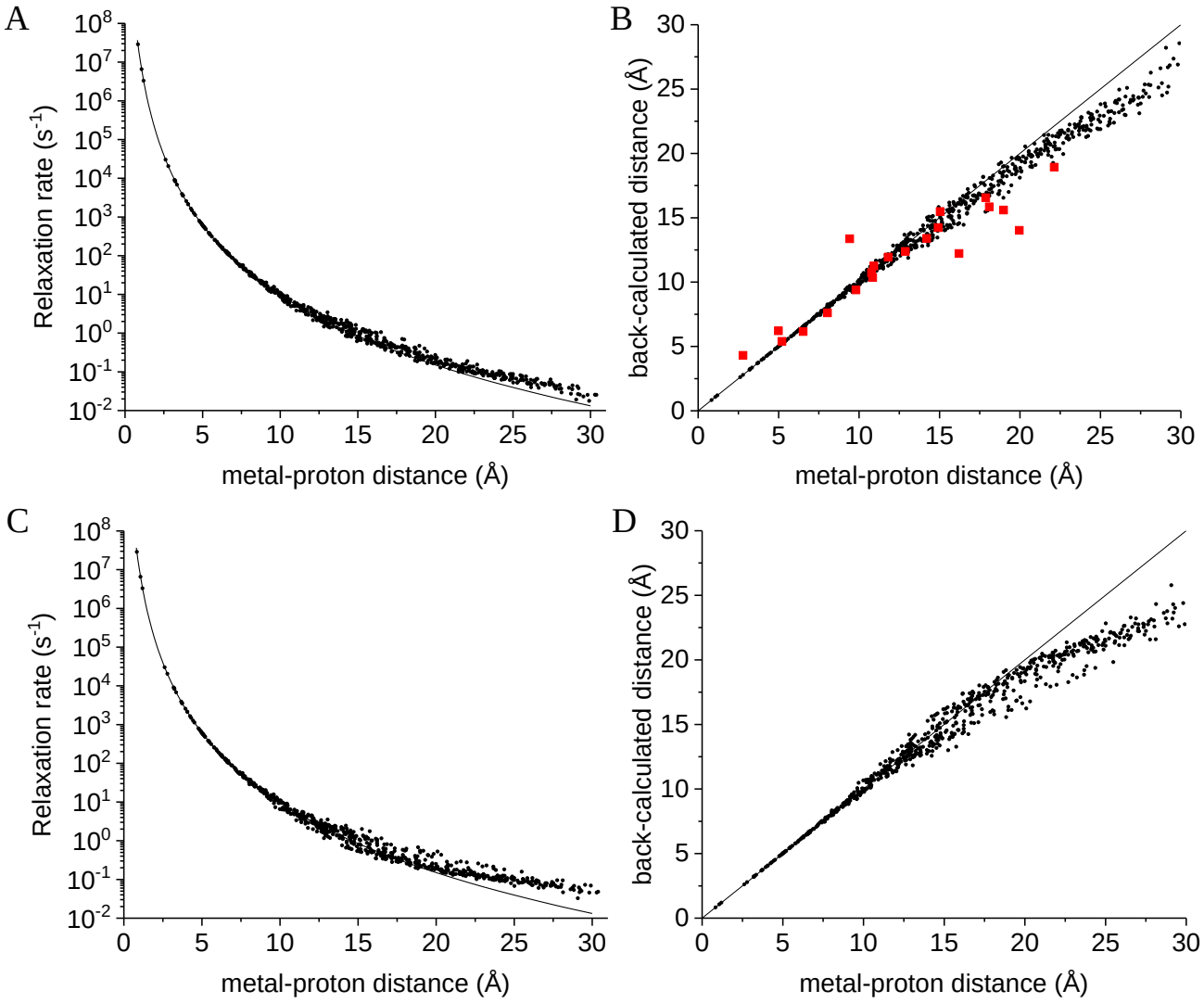

Figure 1. (A) Apparent ~~P~~paramagnetic relaxation rates calculated at 500 MHz for Cu^{2+}-plastocyanin protons. The line indicates the rates predicted with the Solomon equation. (B) Agreement between metal-proton distances as measured in the PDB 2GIM structure and back-calculated from the predicted R_1. (C-D) The same calculations are performed assuming fixed positions for methyl protons. The red points in panel B refer to the distances back-calculated from the experimental data (Ma et al., 2000).

3.2 Solvent water proton relaxation enhancement

The enhancement in nuclear relaxation calculated for protons at large distances from the paramagnetic metal can have important consequences also for the relaxation rate of solvent water protons in solutions containing paramagnetic macromolecules. As a test system, a synthetic model was used mimicking a sphere of hydrogen-bonded water molecules (arranged as in crystalline ice), with a gadolinium(III) ion in the center. In this model, each proton has another proton at about 1.5 Å, and 8 protons between 2.5 and 3.1 Å, for a total of 844 protons. The electron relaxation of gadolinium is calculated assuming typical values for the electron relaxation parameters, Δ_t =0.030 cm^{-1} and τ_v = 20 ps (Caravan et al., 1999; Li et al., 2002; Mastarone et al., 2011), which provide electron relaxation times of 4.2 ns at 1 T and 36 ns at 3 T.

Figure S~~2~~4 shows the magnetization recovery curves for protons at different distances from the gadolinium(III) ion after a 90° pulse; the figure shows that for some nuclei there can be a deviation from a monoexponential function of time. The relaxation rates can however be calculated as rate constants of the monoexponential time-dependence of the magnetization. These rates were first evaluated at 1 and 3 T, for reorientation times of 50, 500 and 5000 ns, for all protons within the sphere, in the absence of chemical exchange with bulk water molecules (Fig. 2). Fig. 2 also shows how the relaxation rates of protons relatively far from the metal increase with respect to the rates calculated from the Solomon equation (Eq. 2). This effect is of increasing importance with increasing the reorientation time of the molecule, the magnetic field (from 1 to 3 T), and the electron relaxation time (Fig. S~~3~~5). In the absence of chemical exchange, and neglecting outer-sphere relaxation mechanisms (Freed, 1978), the relaxation rate of bulk water protons does not change with respect to the intrinsic water molecule relaxation value, ρ_B, fixed to 0.3 s^{-1}.

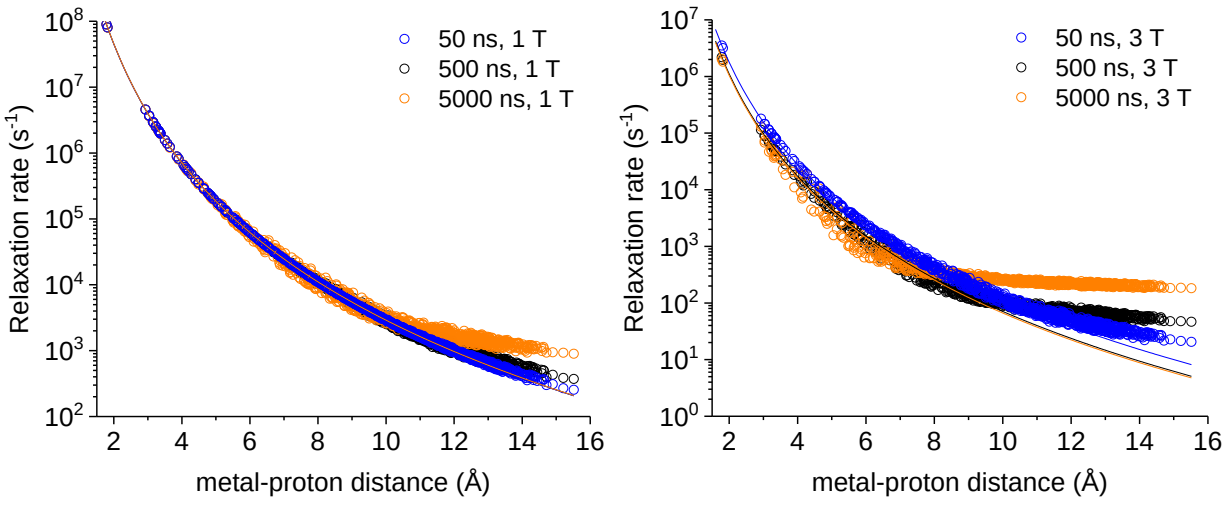

Figure 2. Apparent ~~R~~relaxation rates calculated at 1 T (left panel) and 3 T (right panel) for protons at different distance from a Gd^{3+} ion in the macromolecular model with reorientation time of 50, 500 or 5000 ns. The lines indicate the Solomon relaxation rates calculated for the same reorientation times (colored accordingly).

The effect of this relaxation enhancement on the solvent water proton R_1 was then evaluated in the presence of 100 superficial protons with an exchange rate of 10^4 s^{-1}~~0.1 ms~~. The molar ratio f between the macromolecular concentration and the solvent water proton concentration is assumed equal to 9×10^{-6}, corresponding to a macromolecular concentration of 0.001 mol dm^{-3}. The presence of these exchangeable protons causes a relaxation enhancement of bulk water protons, shown in Fig. 3A. This enhancement increases with increasing the reorientation time of the macromolecule, and for reorientation times of microseconds or larger it largely exceeds the paramagnetic enhancement calculated with the Solomon equation and 100 protons at the same distance from the gadolinium ion and with the same exchange rate. Of note, for so large reorientation times (and lack of any internal mobility), the paramagnetic enhancement can almost reach the values achieved at the same fields by small complexes with a water molecule coordinated to the gadolinium ion and used in MRI (as Gd-DOTA or Gd-DTPA) (Anelli et al., 2000; Caravan et al., 1999; Fragai et al., 2019).

Fig. 3B shows the dependence of the bulk water proton relaxation rate on the exchange rate of the 100 exchangeable surface protons. Sizable paramagnetic enhancements can be achieved for exchange times shorter than milliseconds; the enhancement increases with decreasing the exchange time until a value of the order of the macromolecular reorientation time is reached.

The same model was used to evaluate the bulk water proton relaxation enhancement obtained in the presence of paramagnetic metal ions other than gadolinium. Interestingly, the effect is similar even for S = 1/2 ions with, e.g., an electron relaxation time of 4 ns, i.e. of the order of magnitude typical of type 2 copper(II). Indeed, the paramagnetic relaxation enhancements are about halved at 1 T, but very similar to those calculated for Gd^{3+} at 3 T (see Fig. S~~4~~6).

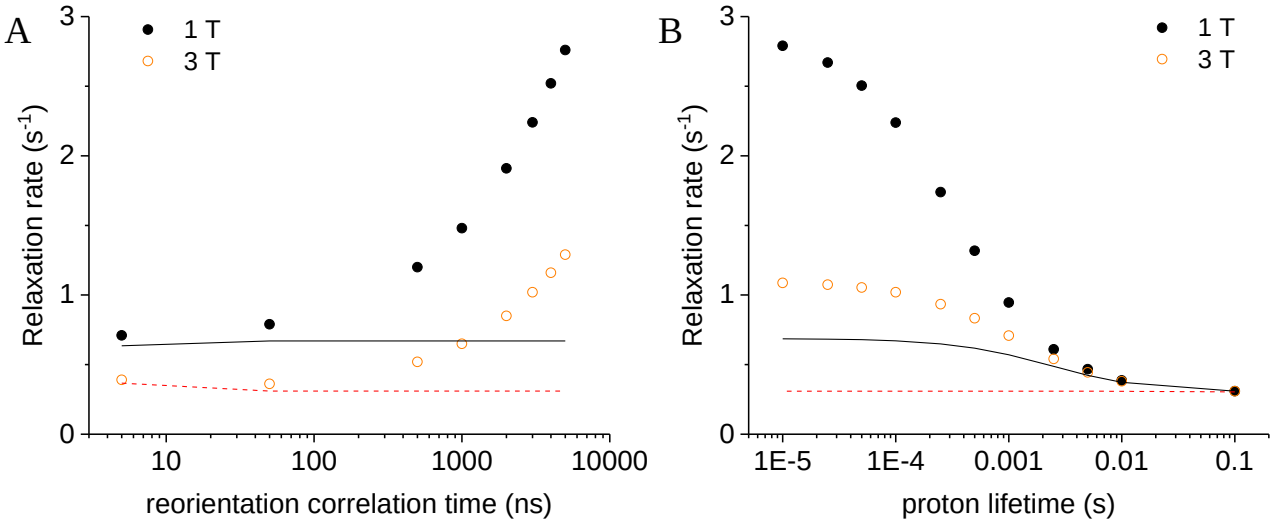

Figure 3. (A) Bulk water proton relaxation rates calculated at 1 and 3 T as a function of the reorientation time of the Gd^{3+}-containing macromolecular model (at 0.001 mol dm^{-3} concentration), with 100 surface protons with exchange rate of 0.1 ms. (B) Bulk water proton

relaxation rates calculated at 1 and 3 T as a function of the exchange rate of 100 surface protons in the macromolecular model with reorientation time of 3000 ns. The bulk water proton relaxation rates calculated with the Solomon equation, and according to $R_{1\mathrm{bulk}} = R_{1\mathrm{dia}} + f(R_{1M}^{-1} + \tau_M)^{-1}$, at 1 and 3 T are shown as solid and dashed lines, respectively. In all calculations, an intrinsic diamagnetic rate of 0.3 s^{-1} is assumed.

In a second synthetic model, a gadolinium(III) ion is placed in the center of a sphere with 6 protons in octahedral geometry at a distance of 2.5 Å from the metal, each proton having further other 6 protons in octahedral geometry at the same distance, and so on. The farther protons are at a distance of 20 Å from the metal. Hundred protons on the surface of the sphere are assumed exchangeable with an exchange rate of 0.1 ms. The relaxation enhancement of bulk water protons again increases significantly for reorientation times longer than microseconds, exceeding of about a factor 10 the paramagnetic enhancement calculated with the Solomon equation due to the same 100 protons, at the same distance from the gadolinium ion and with the same exchange rate (Fig. S~~5~~7).

4 Conclusions

The calculations performed indicate that the magnetization transfer from protons in a polymer matrix to water protons may provide valuable contributions to the water proton relaxation rates in the presence of a paramagnetic metal ion entrapped within the polymer (Rammohan et al., 2016; Ravera et al., 2020; Rotz et al., 2015). This contribution occurs when a paramagnetic metal ion is bound to a rigid macromolecule, composed of a network of hydrogen nuclei few Å away from one another, with microsecond tumbling time, and with hundreds of nuclei in the external layer in relatively fast exchange (tens to hundreds of microseconds) with bulk water protons. These conditions seem hard to meet experimentally, so that this effect cannot be easily exploited for increasing the effectiveness and the safety of a MRI contrast agents. Nevertheless, it might prove useful when the paramagnetic ions are entrapped in slow-rotating proton-rich nanoparticles with sponge-like structures, allowing a large number of exchangeable surface protons, like Gd-based mesoporous silica nanoparticles (Carniato et al., 2018).

Importantly, these calculations also show that assuming a metal-proton distance dependence as r^{-6} for the longitudinal relaxation rates of protons at more than 15 Å from the metal in a macromolecule can originate sizable errors. This should be taken into account when R_1-derived distance restraints are used in structural determination procedures.

Author contribution: CL conceived the project and CL, GP, ER, MF and MB discussed all theoretical aspects and simulations. GB and GP developed the model code and GP, GB, ER and VC performed the simulations. GP prepared the manuscript with contributions from all co-authors.

Competing interests: The authors declare that they have no conflict of interest.

Acknowledgments

CL warmly acknowledges the many friendly discussions over the years with the late Jens J. Led. The authors acknowledge for the financial support the MIUR PRIN 2017A2KEPL and the Fondazione Cassa di Risparmio di Firenze. The work was carried out within the framework of the COST CA15209 Action.

References

Aime, S., Crich, S. G., Gianolio, E., Giovenzana, G. B., Tei, L. and Terreno, E.: High sensitivity lanthanide(III) based probes for MR-medical imaging, Coordination Chemistry Reviews, 250(11), 1562–1579, https://doi.org/10.1016/j.ccr.2006.03.015, 2006.

Aime, S., Botta, M., Esteban-Gómez, D. and Platas-Iglesias, C.: Characterisation of magnetic resonance imaging (MRI) contrast agents using NMR relaxometry, Molecular Physics, 117(7–8), 898–909, https://doi.org/10.1080/00268976.2018.1516898, 2019.

Anelli, P. L., Bertini, I., Fragai, M., Lattuada, L., Luchinat, C. and Parigi, G.: Sulfonamide-Functionalized Gadolinium DTPA Complexes as Possible Contrast Agents for MRI: A Relaxometric Investigation, European Journal of Inorganic Chemistry, 2000(4), 625–630, https://doi.org/10.1002/(SICI)1099-0682(200004)2000:4<625::AID-EJIC625>3.0.CO;2-2, 2000.

Balayssac, S., Bertini, I., Bhaumik, A., Lelli, M. and Luchinat, C.: Paramagnetic shifts in solid-state NMR of proteins to elicit strucutral information., Proc.Natl.Acad.Sci.USA, 105, 17284–17289, 2008.

Banci, L. and Luchinat, C.: Selective versus non-selective T1 experiments to determine metal-nucleus distances in paramagnetic proteins, Inorganica Chimica Acta, (275–276), 373–379, 1998.

Benda, L., Mareš, J., Ravera, E., Parigi, G., Luchinat, C., Kaupp, M. and Vaara, J.: Pseudo-Contact NMR Shifts over the Paramagnetic Metalloprotein CoMMP-12 from First Principles, Angew. Chem. Int. Ed. Engl., 55(47), 14713–14717, https://doi.org/10.1002/anie.201608829, 2016.

Bertini, I., Luchinat, C., Parigi, G. and Ravera, E.: NMR of paramagnetic molecules: applications to metallobiomolecules and models., 2017.

Boelens, R., Koning, T. M. G., Van der Marel, G. A., Van Boom, J. H. and Kaptein, R.: Iterative procedure for structure determination from proton-proton NOEs using a full relaxation matrix approach. Application to a DNA octamer, J.Magn.Reson., 82, 290–308, 1989.

Borgias, B., Thomas, P. D. and James, T. L.: COmplete Relaxation Matrix Analysis (CORMA)., University of California, San Francisco, CA., 1989.

Caravan, P., Ellison, J. J., McMurry, T. J. and Lauffer, R. B.: Gadolinium(III) chelates as MRI contrast agents: structure, dynamics, and applications, Chem.Rev., 99, 2293–2351, 1999.

Carniato, F., Tei, L. and Botta, M.: Gd-Based Mesoporous Silica Nanoparticles as MRI Probes, European Journal of Inorganic Chemistry, 2018(46), 4936–4954, https://doi.org/10.1002/ejic.201801039, 2018.

Fragai, M., Ravera, E., Tedoldi, F., Luchinat, C. and Parigi, G.: Relaxivity of Gd-Based MRI Contrast Agents in Crosslinked Hyaluronic Acid as a Model for Tissues, ChemPhysChem, 20(17), 2204–2209, https://doi.org/10.1002/cphc.201900587, 2019.

Freed, J. H.: Dynamic effects of pair correlation functions on spin relaxation by translational diffusion in liquids. II. Finite jumps and independent T_1 processes, The Journal of Chemical Physics, 68(9), 4034–4037, https://doi.org/10.1063/1.436302, 1978.

Jayalakshmi, V. and Rama Krishna, N.: Complete Relaxation and Conformational Exchange Matrix (CORCEMA) Analysis of Intermolecular Saturation Transfer Effects in Reversibly Forming Ligand–Receptor Complexes, Journal of Magnetic Resonance, 155(1), 106–118, https://doi.org/10.1006/jmre.2001.2499, 2002.

Koenig, S. H. and Brown III, R. D.: Field-Cycling Relaxometry of Protein Solutions and Tissue: Implications for MRI, Progress in Nuclear Magnetic Resonance Spectroscopy, 22, 487–567, 1990.

Li, C., Parigi, G., Fragai, M., Luchinat, C. and Meade, T. J.: Mechanistic studies of a calcium-dependent MRI contrast agent, Inorganic Chemistry, 41, 4018–4024, 2002.

Libralesso, E., Nerinovski, K., Parigi, G. and Turano, P.: 1H nuclear magnetic relaxation dispersion of Cu,Zn superoxide dismutase in the native and guanidinium-induced unfolded forms, Biochem.Biophys.Res.Commun., 328, 633–639, 2005.

Ma, L., Jorgensen, A. M. M., Sorensen, G. O., Ulstrup, J. and Led, J. J.: Elucidation of the Paramagnetic R1 Relaxation of Heteronuclei and Protons in Cu(II) Plastocyanin from Anabaena variabilis, Journal of the American Chemical Society, 122, 9473–9485, 2000.

Mastarone, D. J., Harrison, V. S. R., Eckermann, A. L., Parigi, G., Luchinat, C. and Meade, T. J.: A Modular System for the Synthesis of Multiplexed Magnetic Resonance Probes, Journal of the American Chemical Society, 133(14), 5329–5337, https://doi.org/10.1021/ja1099616, 2011.

Neuhaus, D. and Williamson, M. P.: The Nuclear Overhauser Effect in Structural and Conformational Analysis, VCH Publisher, Inc., 1989.

Olejniczak, E. T., Gampe, R. T. and Fesik, S. W.: Accounting for spin diffusion in the analysis of 2D NOE data, Journal of Magnetic Resonance (1969), 67(1), 28–41, https://doi.org/10.1016/0022-2364(86)90406-3, 1986.

Post, C. B., Meadows, R. P. and Gorenstein, D. G.: On the evaluation of interproton distances for three-dimensional structure determination by NMR using a relaxation rate matrix analysis, J. Am. Chem. Soc., 112(19), 6796–6803, https://doi.org/10.1021/ja00175a009, 1990.

Rammohan, N., MacRenaris, K. W., Moore, L. K., Parigi, G., Mastarone, D. J., Manus, L. M., Lilley, L. M., Preslar, A. T., Waters, E. A., Filicko, A., Luchinat, C., Ho, D. and Meade, T. J.: Nanodiamond–Gadolinium(III) Aggregates for Tracking Cancer Growth In Vivo at High Field, Nano Letters, 16(12), 7551–7564, https://doi.org/10.1021/acs.nanolett.6b03378, 2016.

Ravera, E., Parigi, G., Mainz, A., Religa, T. L., Reif, B. and Luchinat, C.: Experimental Determination of Microsecond Reorientation Correlation Times in Protein Solutions, J. Phys. Chem. B, 117(13), 3548–3553, https://doi.org/10.1021/jp312561f, 2013.

Ravera, E., Fragai, M., Parigi, G. and Luchinat, C.: Different flavors of diffusion in paramagnetic systems: Unexpected NMR signal intensity and relaxation enhancements, Journal of Magnetic Resonance Open, 2–3, 100003, https://doi.org/10.1016/j.jmro.2020.100003, 2020.

Rotz, M. W., Culver, K. S. B., Parigi, G., MacRenaris, K. W., Luchinat, C., Odom, T. W. and Meade, T. J.: High Relaxivity Gd(III)–DNA Gold Nanostars: Investigation of Shape Effects on Proton Relaxation, ACS Nano, 9(3), 3385–3396, https://doi.org/10.1021/nn5070953, 2015.

Solomon, I.: Relaxation Processes in a System of Two Spins, Phys. Rev., 99(2), 559–565, https://doi.org/10.1103/PhysRev.99.559, 1955.

Wahsner, J., Gale, E. M., Rodríguez-Rodríguez, A. and Caravan, P.: Chemistry of MRI Contrast Agents: Current Challenges and New Frontiers, Chemical Reviews, 119(2), 957–1057, https://doi.org/10.1021/acs.chemrev.8b00363, 2019.

Revisiting paramagnetic relaxation enhancements in slowly rotating systems: how long is the long range?

Giovanni Bellomo[1,2,$], Enrico Ravera[1,2], Vito Calderone[1,2], Mauro Botta[3], Marco Fragai[1,2], Giacomo Parigi[1,2], Claudio Luchinat[1,2]

[1]Magnetic Resonance Center (CERM) and Department of Chemistry, University of Florence, via Sacconi 6, Sesto Fiorentino, Italy

[2]Consorzio Interuniversitario Risonanze Magnetiche di Metalloproteine (CIRMMP), Sesto Fiorentino, Italy

[3]Dipartimento di Scienze e Innovazione Tecnologica, Università del Piemonte Orientale "Amedeo Avogadro", Viale T. Michel 11, 15121, Alessandria, Italy

[$]Present address: Laboratory of Clinical Neurochemistry, Neurology Clinic, University of Perugia, Piazzale Lucio Severi 1/8, 06132 Perugia (PG), Italy

Correspondence to: Claudio Luchinat (luchinat@cerm.unifi.it)

SUPPLEMENT

The complete relaxation rate-matrix approach

The time dependence of the longitudinal magnetization due to the dipole-dipole interaction between two magnetically unlike spins I and J of equal spin quantum number ($I = J$) is described by (Bertini et al., 2017; Solomon, 1955)

$$\frac{\mathrm{d}M_z^I}{\mathrm{d}t} = -\rho^I \left(M_z^I - M_{eq}^I\right) - \sigma^{IJ}\left(M_z^J - M_{eq}^J\right) \tag{S1a}$$

$$\frac{\mathrm{d}M_z^J}{\mathrm{d}t} = -\rho^J \left(M_z^J - M_{eq}^J\right) - \sigma^{JI}\left(M_z^I - M_{eq}^I\right) \tag{S1b}$$

where M_{eq} is the equilibrium magnetization, with

$$\rho^I = w_0 + 2w_1^I + w_2 \tag{S2a}$$

$$\rho^J = w_0 + 2w_1^J + w_2 \tag{S2b}$$

$$\sigma^{IJ} = \sigma^{JI} = w_2 - w_0\,. \tag{S3}$$

The terms w_0, w_1 and w_2 indicate the zero, single and double quantum spin transition probabilities, respectively: w_0 is the probability of transition simultaneously causing a decrease in m_I and an increase in m_J, or vice versa (zero quantum transitions), and is equal to

$$w_0 = \frac{2}{15}\left(\frac{\mu_0}{4\pi}\frac{\hbar^2\gamma_I\gamma_J}{r_{IJ}^3}\right)^2 J(J+1)\frac{\tau_c}{1+(\omega_I-\omega_J)^2\tau_c^2} \tag{S4}$$

where r_{IJ} is the internuclear distance; w_1^I is the probability of single transitions between states with the same m_J and different m_I (single quantum transitions)

$$w_1^I = \frac{1}{5}\left(\frac{\mu_0}{4\pi}\frac{\hbar^2\gamma_I\gamma_J}{r_{IJ}^3}\right)^2 J(J+1)\frac{\tau_c}{1+\omega_I^2\tau_c^2} \tag{S5}$$

and w_2 indicates the probabilities of transitions causing a decrease, or an increase, in both m_I and m_J (double quantum transitions)

$$w_2 = \frac{4}{5}\left(\frac{\mu_0}{4\pi}\frac{\hbar^2\gamma_I\gamma_J}{r_{IJ}^3}\right)^2 J(J+1)\frac{\tau_c}{1+(\omega_I+\omega_J)^2\tau_c^2} \quad \text{(S6)}$$

In the assumption of a completely rigid spherical molecule, the correlation time τ_c is the isotropic molecular reorientation time.

The cross relaxation rates $\sigma^{IJ} = \sigma^{JI}$ describe the effect on the variation of the magnetization of one spin due to the variation of the magnetization of the other spin, resulting from their interaction.

By definition of a magnetization vector $\mathbf{M} = \begin{pmatrix} M_z^I \\ M_z^J \end{pmatrix}$ and of a relaxation matrix $\mathbf{R} = \begin{pmatrix} \rho^I & \sigma^{IJ} \\ \sigma^{JI} & \rho^J \end{pmatrix}$,

Eqs. 1 can be written in the matrix form

$$\frac{\mathrm{d}\mathbf{M}}{\mathrm{d}t} = -\mathbf{R}\cdot\left(\mathbf{M} - \mathbf{M_{eq}}\right) \quad \text{(S7)}$$

so that

$$\mathbf{M}(t) - \mathbf{M_{eq}} = \exp(-\mathbf{R}t)\cdot(\mathbf{M}(0) - \mathbf{M_{eq}}) \quad \text{(S8)}$$

In the presence of a rigid macromolecule with N atoms of the ^{1}H nuclide, the relaxation matrix becomes

$$\mathbf{R} = \begin{pmatrix} \rho_1 & \sigma_{12} & \sigma_{13} & \cdots & \sigma_{1N} \\ \sigma_{12} & \rho_2 & \sigma_{23} & \cdots & \sigma_{2N} \\ \sigma_{13} & \sigma_{23} & \rho_3 & \cdots & \sigma_{3N} \\ \vdots & \vdots & \vdots & \cdots & \vdots \\ \sigma_{1N} & \sigma_{2N} & \sigma_{3N} & \cdots & \rho_N \end{pmatrix} \quad \text{(S9)}$$

where

$$\rho_i = \sum_{j=1, j\neq i}^{N} \rho_{ij} \quad \text{(S10)}$$

with (see Eqs. 2)

$$\rho_{ij} = \frac{2}{15}\left(\frac{\mu_0}{4\pi}\frac{\hbar\gamma_I^2}{r_{ij}^3}\right)^2 I(I+1)\left[\tau_c + \frac{3\tau_c}{1+\omega_I^2\tau_c^2} + \frac{6\tau_c}{1+4\omega_I^2\tau_c^2}\right] \quad \text{(S11)}$$

if the *i*th and *j*th spin systems are magnetically non-equivalent (unlike spins), or by

$$\rho_{ij} = \frac{2}{5}\left(\frac{\mu_0}{4\pi}\frac{\hbar\gamma_I^2}{r_{ij}^3}\right)^2 I(I+1)\left[\frac{\tau_c}{1+\omega_I^2\tau_c^2} + \frac{4\tau_c}{1+4\omega_I^2\tau_c^2}\right] \tag{S12}$$

(corresponding to $\rho^I + \sigma^{IJ}$, see Eqs. 2a and 3), if *i*th and *j*th spin systems are magnetically equivalent (like spins), as, e.g., the methyl protons. The off-diagonal elements are

$$\sigma_{ij} = \frac{2}{15}\left(\frac{\mu_0}{4\pi}\frac{\hbar\gamma_I^2}{r_{ij}^3}\right)^2 I(I+1)\left[\frac{6\tau_c}{1+4\omega_I^2\tau_c^2} - \tau_c\right] \tag{S13}$$

Since **R** is a symmetric matrix, it can be diagonalized and written in the form

$$\mathbf{R} = \boldsymbol{\chi}\cdot\boldsymbol{\lambda}\cdot\boldsymbol{\chi}^{-1} \tag{S14}$$

where $\boldsymbol{\lambda}$ is the diagonal matrix of eigenvalues and $\boldsymbol{\chi}$ is the unitary eigenvector matrix. The program CORMA (Borgias et al., 1989) can be used to perform these calculations by providing the macromolecular structure in input.

From Eqs. 8 and 14, the time dependence of the *z*-component of the magnetization of each nuclear spin of the macromolecule can be calculated from the expression

$$\mathbf{M}(t) - \mathbf{M_{eq}} = \boldsymbol{\chi}\cdot\exp(-\boldsymbol{\lambda}t)\cdot\boldsymbol{\chi}^{-1}\cdot(\mathbf{M}(0) - \mathbf{M_{eq}}) \tag{S15}$$

where

$$\exp(-\boldsymbol{\lambda}t) = \begin{pmatrix} \exp(-\lambda_1 t) & 0 & 0 & \dots & 0 \\ 0 & \exp(-\lambda_2 t) & 0 & \dots & 0 \\ 0 & 0 & \exp(-\lambda_3 t) & \cdots & 0 \\ \vdots & \vdots & \vdots & \cdots & \vdots \\ 0 & 0 & 0 & \cdots & \exp(-\lambda_N t) \end{pmatrix}$$

with λ_i being the eigenvalues of the matrix **R**.

In the presence of chemical exchange, in the limiting case of a single nucleus in chemical exchange with bulk solvent nuclei,

$$I_1 \underset{k_{-1}}{\overset{k_1}{\rightleftharpoons}} I_B$$

the time evolution of the longitudinal magnetization is given by

$$\frac{d}{\mathrm{d}t}\begin{pmatrix} M_z^I \\ M_z^B \end{pmatrix} = -\begin{pmatrix} \rho_1^I + k_1 & -k_{-1} \\ -k_1 & \rho_B + k_{-1} \end{pmatrix}\begin{pmatrix} M_z^I - M_{eq}^I \\ M_z^B - M_{eq}^B \end{pmatrix}$$

and since at equilibrium $k_1 P_1 = k_{-1} P_B$ (P_1 is the population of the nuclei in position 1 and in the bulk), it results that $\frac{k_{-1}}{k_1} = \frac{P_1}{P_B} = f$.

The relaxation rates of the solvent molecule nuclei interacting with the macromolecule and of the bulk solvent molecule nuclei can be calculated by including in the relaxation matrix as many extra rows and columns as the number of nuclei belonging to the interacting solvent molecules, and an additional row and column relative to bulk solvent nuclei. Assuming M solvent nuclei interacting with the macromolecule (composed of N nuclei), the relaxation matrix becomes

$$\mathbf{R} = \begin{pmatrix} \rho_1 + k_1 + R_{1M,1} & \sigma_{12} & \cdots & \sigma_{1N} & \sigma_{1(N+1)} & \cdots & \sigma_{1(N+M)} & -fk_1 \\ \sigma_{12} & \rho_2 + k_2 + R_{1M,2} & \cdots & \sigma_{2N} & \sigma_{2(N+1)} & \cdots & \sigma_{2(N+M)} & -fk_2 \\ \vdots & \vdots & \ddots & \vdots & \vdots & \ddots & \vdots & \vdots \\ \sigma_{1N} & \sigma_{2N} & \cdots & \rho_N + k_N + R_{1M,N} & \sigma_{N(N+1)} & \cdots & \sigma_{N(N+M)} & -fk_N \\ \sigma_{1(N+1)} & \sigma_{2(N+1)} & \cdots & \sigma_{N(N+1)} & \rho_{N+1} + k_{N+1} + R_{1M,N+1} & \cdots & \sigma_{(N+1)(N+M)} & -fk_{N+1} \\ \vdots & \vdots & \ddots & \vdots & \vdots & \ddots & \vdots & \vdots \\ \sigma_{1(N+M)} & \sigma_{2(N+M)} & \cdots & \sigma_{N(N+M)} & \sigma_{(N+1)(N+M)} & \cdots & \rho_{N+M} + k_{N+M} + R_{1M,N+M} & -fk_{N+M} \\ -k_1 & -k_2 & \cdots & -k_N & -k_{N+1} & \cdots & -k_{N+M} & \rho_B + f\sum_i k_i \end{pmatrix} \quad \text{(S16)}$$

where $k_i = \left(\tau_{M,i}\right)^{-1}$ are the exchange rate constants, f is the ratio between the macromolecular concentration and the solvent molecule nuclei concentration, and ρ_B is the relaxation rate of bulk solvent nuclei in the absence of the macromolecule. The coefficient f in the last column originates from the relationship $k_{-i} = f k_i$ (see above).

Finally, using a "normalized" magnetization for the bulk nuclei, $\mathbf{M}' = \begin{pmatrix} M_z^I \\ \vdots \\ fM_z^B \end{pmatrix} = \begin{pmatrix} M_z^I \\ \vdots \\ \widetilde{M}_z^B \end{pmatrix}$, the relaxation matrix becomes

$$\mathbf{R}' = \begin{pmatrix} \rho_1 + k_1 + R_{1M,1} & \sigma_{12} & \cdots & \sigma_{1N} & \sigma_{1(N+1)} & \cdots & \sigma_{1(N+M)} & -k_1 \\ \sigma_{12} & \rho_2 + k_2 + R_{1M,2} & \cdots & \sigma_{2N} & \sigma_{2(N+1)} & \cdots & \sigma_{2(N+M)} & -k_2 \\ \vdots & \vdots & \ddots & \vdots & \vdots & \ddots & \vdots & \vdots \\ \sigma_{1N} & \sigma_{2N} & \cdots & \rho_N + k_N + R_{1M,N} & \sigma_{N(N+1)} & \cdots & \sigma_{N(N+M)} & -k_N \\ \sigma_{1(N+1)} & \sigma_{2(N+1)} & \cdots & \sigma_{N(N+1)} & \rho_{N+1} + k_{N+1} + R_{1M,N+1} & \cdots & \sigma_{(N+1)(N+M)} & -k_{N+1} \\ \vdots & \vdots & \ddots & \vdots & \vdots & \ddots & \vdots & \vdots \\ \sigma_{1(N+M)} & \sigma_{2(N+M)} & \cdots & \sigma_{N(N+M)} & \sigma_{(N+1)(N+M)} & \cdots & \rho_{N+M} + k_{N+M} + R_{1M,N+M} & -k_{N+M} \\ -fk_1 & -fk_2 & \cdots & -fk_N & -fk_{N+1} & \cdots & -fk_{N+M} & \rho_B + f\sum_i k_i \end{pmatrix} \quad \text{(S17)}$$

Bertini, I., Luchinat, C., Parigi, G. and Ravera, E.: NMR of paramagnetic molecules: applications to metallobiomolecules and models., 2017.

Borgias, B., Thomas, P. D. and James, T. L.: COmplete Relaxation Matrix Analysis (CORMA)., University of California, San Francisco, CA., 1989.

Solomon, I.: Relaxation Processes in a System of Two Spins, Phys. Rev., 99(2), 559–565, doi:10.1103/PhysRev.99.559, 1955.

Figure S1 shows the results of calculations for a system of six protons placed along a straight line at 10, 12, 14, 16, 18 and 20 Å from a gadolinium ion. The figure also shows (black dotted lines) the magnetization curves expected from the Solomon equation for the two protons at 10 and 20 Å. Clearly only the first points of the magnetization recovery for the proton at 10 Å agree with the relaxation rate predicted by the Solomon equation. In fact, the magnetization of the proton at 10 Å recovers its equilibrium value slower than predicted from an exponential behavior, so that the monoexponential fit provides a longer relaxation time. On the contrary, the magnetization recovery of the protons at the largest distances is steeper than predicted from an exponential behavior and the relaxation rates are sizably larger than predicted from the Solomon equation.

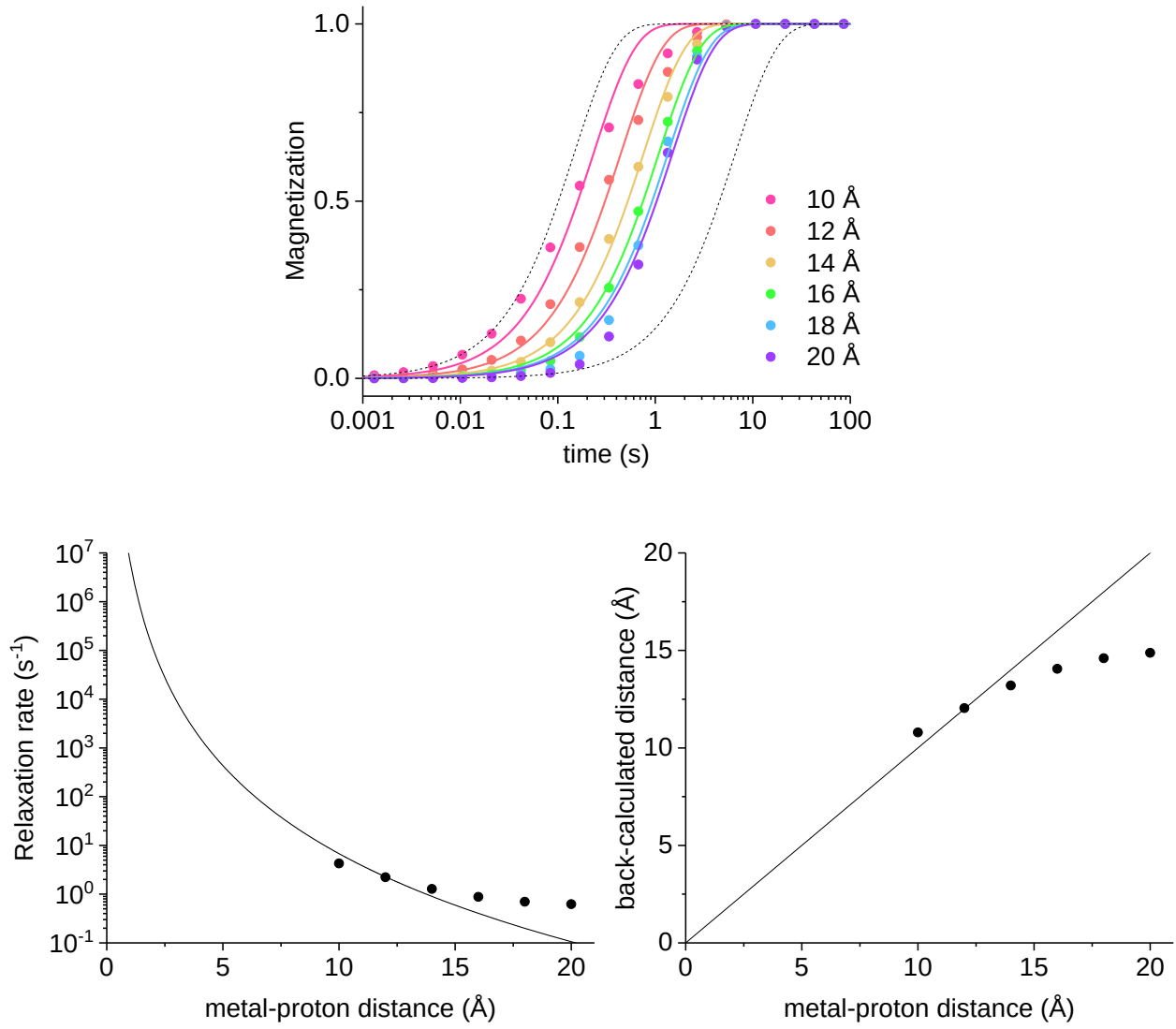

Figure S1. Calculated magnetization recovery for six protons placed along a straight line at 10, 12, 14, 16, 18 and 20 Å from a gadolinium ion, at 700 MHz (upper panel). The black dotted lines show the (monoexponential) behavior predicted from the Solomon equation for the two protons at 10 and 20 Å. The magnetization data calculated for the 6 protons are clearly not monoexponential. The monoexponential fits (solid colored lines) provide the relaxation rates and the back-calculated distances shown in the lower panels.

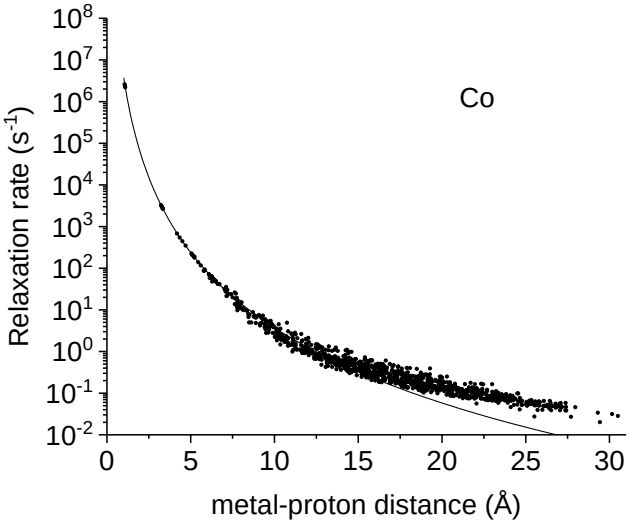
Co
Relaxation rate (s-1)
metal-proton distance (Å)

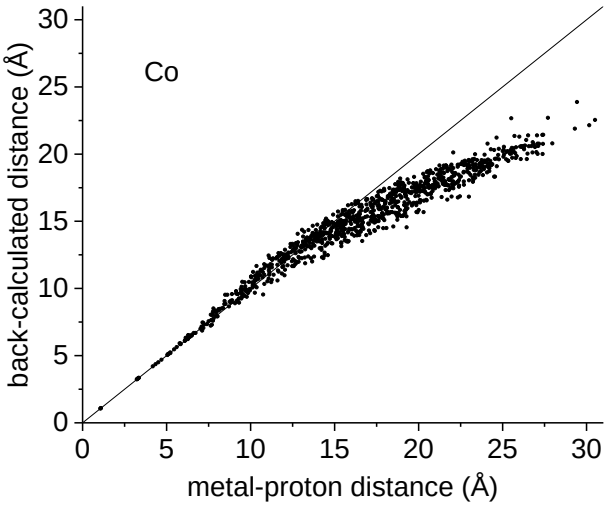
Co
back-calculated distance (Å)
metal-proton distance (Å)

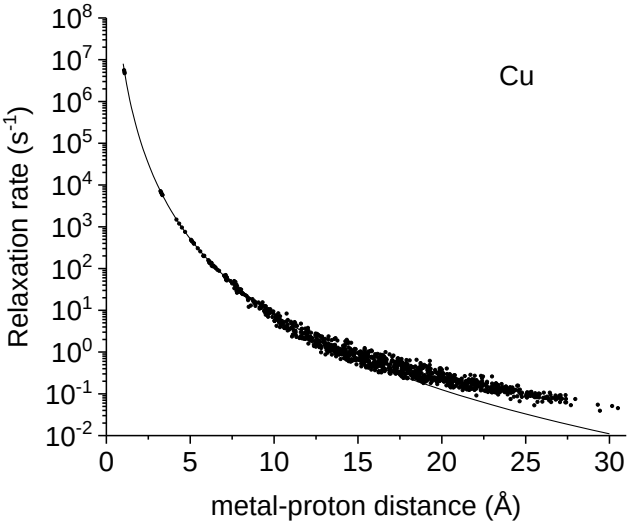
Cu
Relaxation rate (s-1)
metal-proton distance (Å)

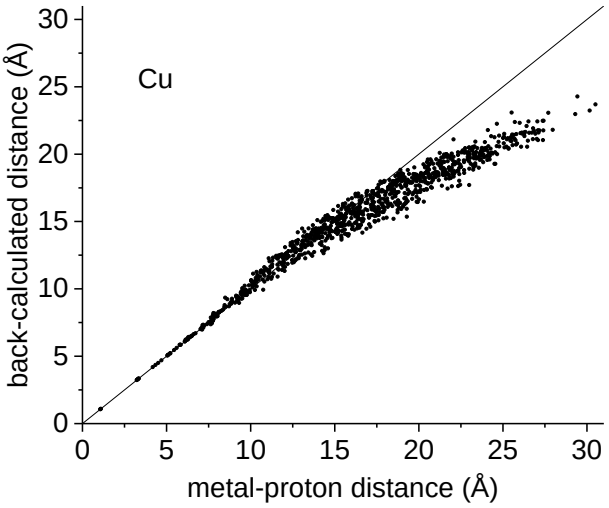
Cu
back-calculated distance (Å)
metal-proton distance (Å)

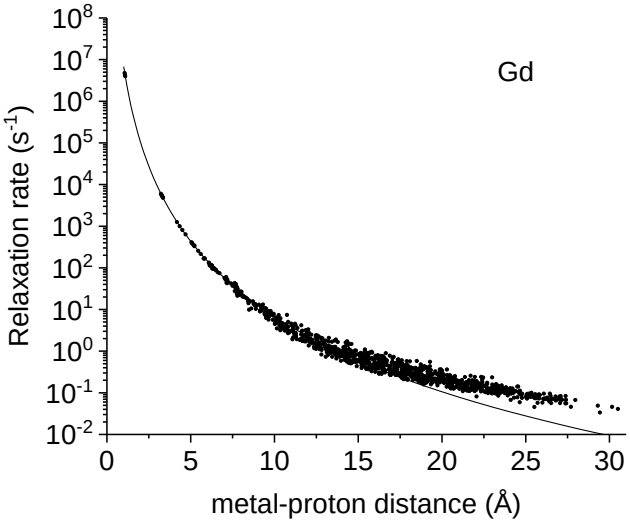
Gd
Relaxation rate (s-1)
metal-proton distance (Å)

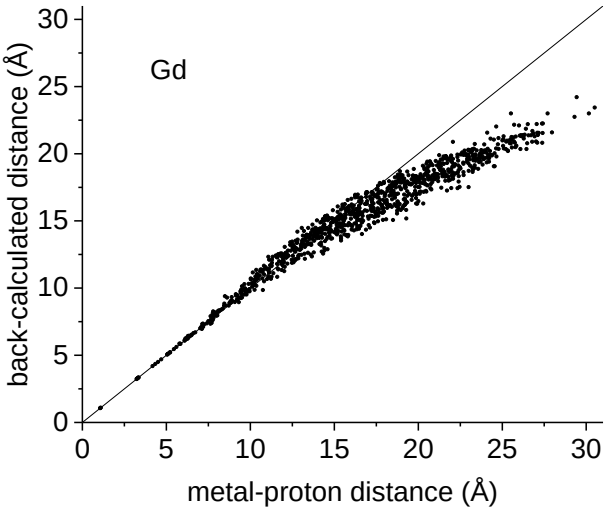
Gd
back-calculated distance (Å)
metal-proton distance (Å)

Figure S2. (left panels) Paramagnetic relaxation rates calculated at 700 MHz for MMP-12 protons, with a reorientation time of 12 ns, in the presence of high spin cobalt(II) (with an electron relaxation rate of 10 ps), copper(II) (with an electron relaxation rate of 0.17 ns), or gadolinium(III) ions (with an electron relaxation rate of 1 μs), replaced to the catalytic zinc(II) ion. The lines indicate the rates predicted with the Solomon equation. (right panels) Agreement between metal-proton distances as measured in the PDB 5LAB structure and back-calculated from the predicted R_1.

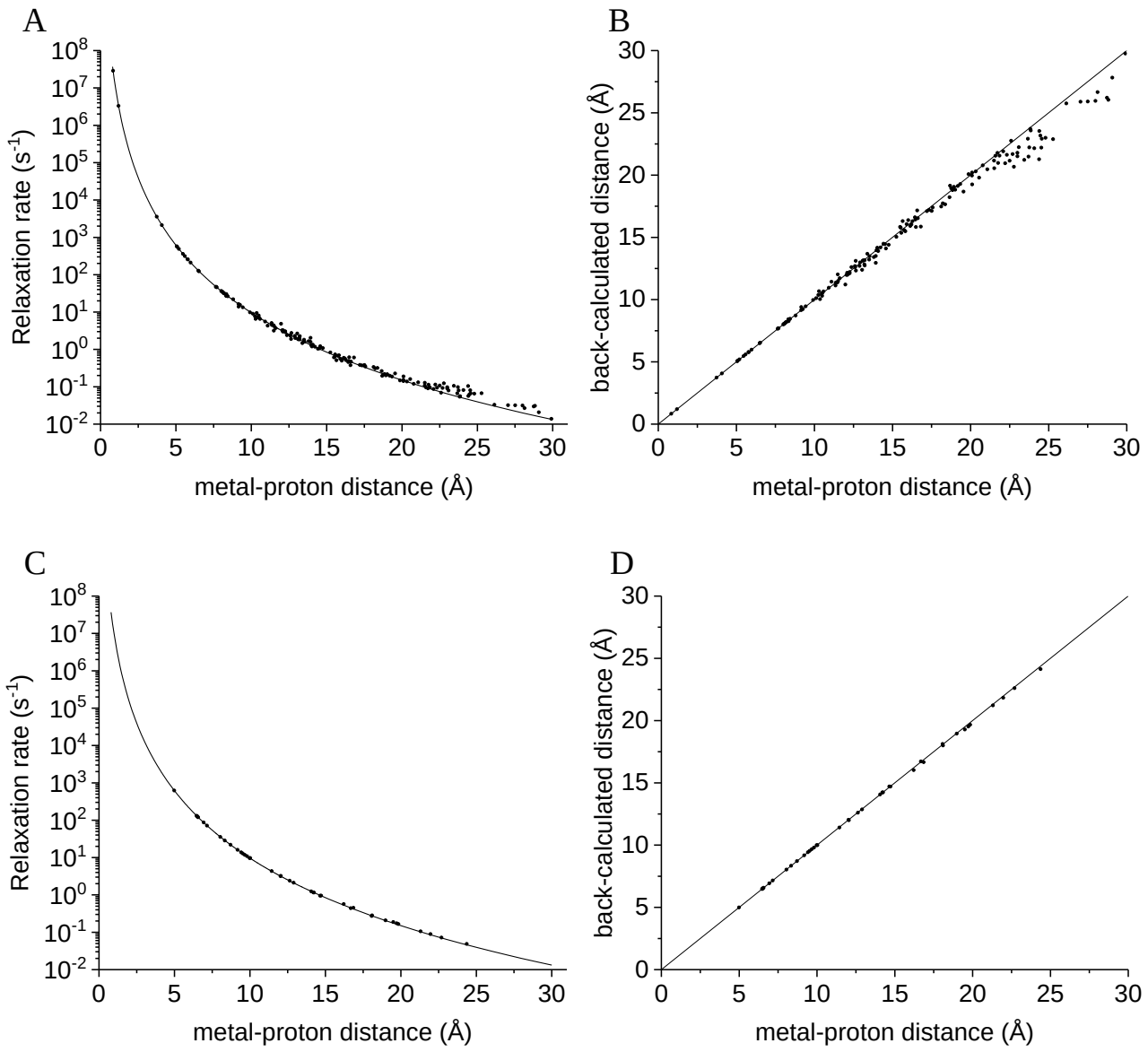

Figure S3. (A) Paramagnetic relaxation rates calculated at 500 MHz for Cu^{2+}-plastocyanin exchangeable (amide and hydroxyl) protons, in perdeuterated conditions. The line indicates the rates predicted with the Solomon equation. (C) Paramagnetic relaxation rates for isoleucine, leucine and valine methyl protons, assuming perdeuteration of all other hydrogens. (B and D) Agreement between metal-proton distances as measured in the PDB 2GIM structure and back-calculated from the predicted R_1 shown in panels A and C, respectively.

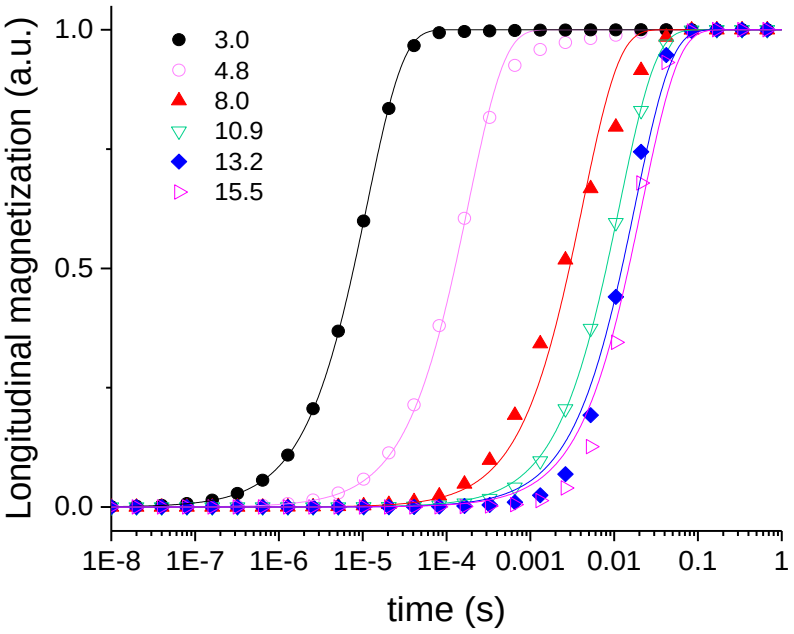

Figure S4. Magnetization recovery after a 90° pulse for protons at 3.0, 4.8, 8.0, 10.9, 13.2 and 15.5 Å from a Gd^{3+} ion, with electron relaxation time of 36 ns, in a macromolecule with a reorientation time of 500 ns, at 3 T. The lines indicate the monoexponential fit of the data.

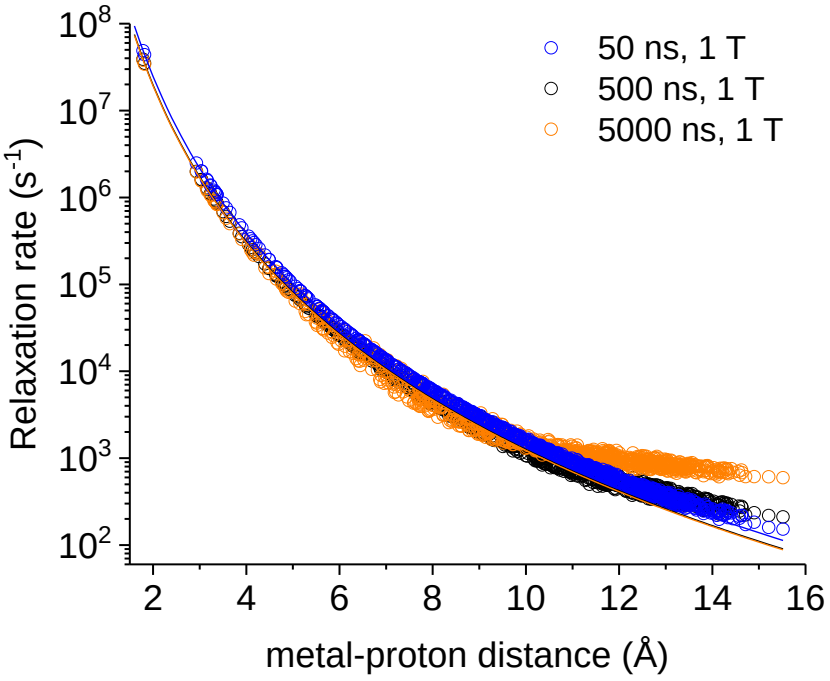

Figure S5. Relaxation rates calculated at 1 T for protons at different distance from a Gd^{3+} ion with electron relaxation time of 17 ns in the macromolecular model with reorientation time of 50, 500 or 5000 ns. The lines indicate the Solomon relaxation rates calculated for the same reorientation times (colored accordingly). The relaxation rate is calculated assuming Δ_t =0.015 cm^{-1} and τ_V= 20 ps, instead of Δ_t =0.030 cm^{-1} and τ_V= 20 ps, that provide 4.2 ns at 1 T.

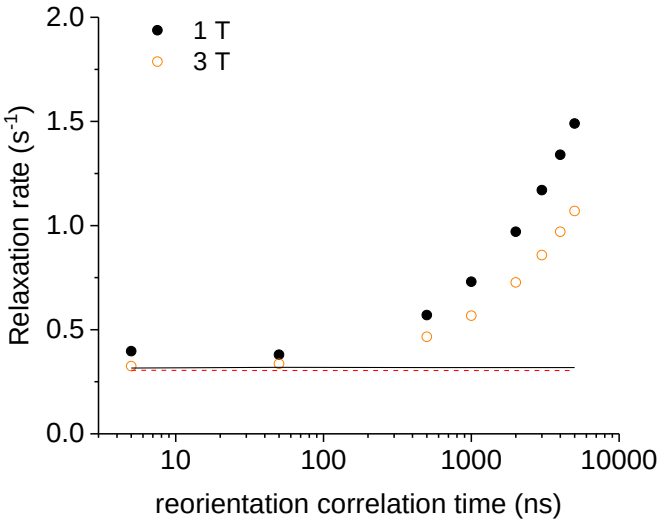

Figure S6. Bulk water proton relaxation rates calculated at 1 and 3 T as a function of the reorientation time of the macromolecular model (at 0.001 mol dm^{-3} concentration) with a $S = 1/2$ ion and electron relaxation time of 4 ns, with 100 surface protons with exchange rate of 0.1 ms. The bulk water proton relaxation rates calculated with the Solomon equation at 1 and 3 T are shown as solid and dashed lines, respectively. In all calculations, an intrinsic diamagnetic rate of 0.3 s^{-1} is assumed.

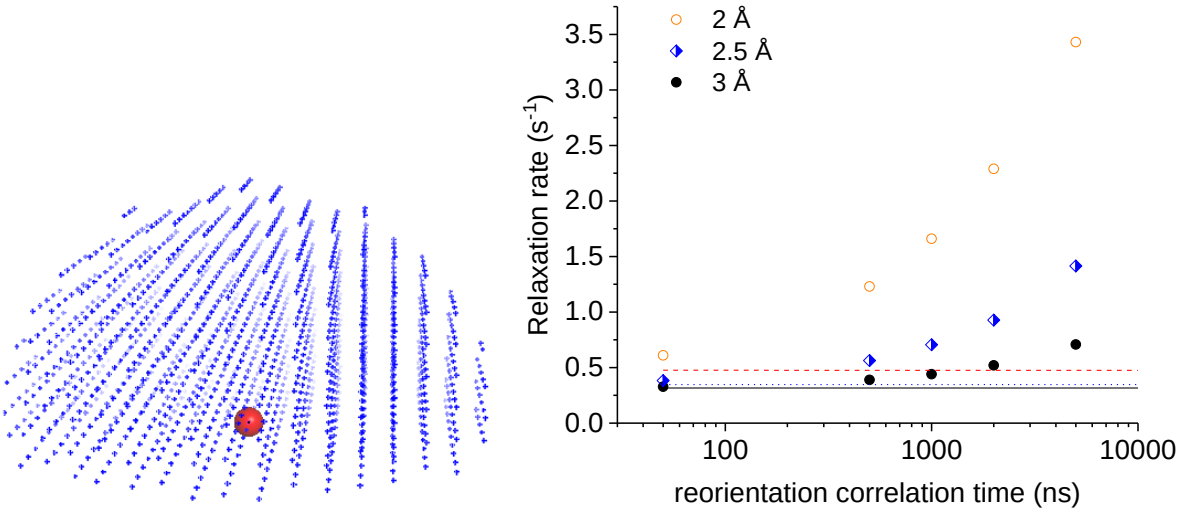

Figure S7. (A) Half-spherical structural model with protons in octahedral geometry and the metal ion (red sphere) in the center. (B) Bulk water proton relaxation rates at 1 T as a function of the reorientation time of a macromolecular sphere containing a Gd^{3+}-ion in the center and protons at distances of 2, 2.5 or 3 Å (see panel A), with 100 surface protons with exchange rate of 0.1 ms. The bulk water proton relaxation rates calculated with the Solomon equation are shown as lines. In all calculations, an intrinsic diamagnetic rate of 0.3 s^{-1} is assumed. The electron relaxation time of gadolinium is calculated assuming the typical values for the electron relaxation parameters, $\Delta_t = 0.030$ cm^{-1} and $\tau_V = 20$ ps.